Dynamic Light Scattering-Assisted Design of an Optimized NiS-ZnS Nanocomposite for Efficient Photocatalytic Dye Degradation: Experimental and Theoretical Insights

Muhammad Younas Afzal[1,2], Muhammad Bilal[2*], Muhammad Asif[2,3], Saeed Rehman[4], Jamshaid Hussain[5], Qing Liu[6], Hamza Khan[1], Nadia Riaz[2], Farooq Ahmad[7], Muhammad Tahir Amin[8***]

Ahson Jabbar Shaikh[1**]

[1]Department of Chemistry, COMSATS University Islamabad, Abbottabad Campus, Abbottabad – 22060, KPK, Pakistan

[2]Department of Environmental Sciences, COMSATS University Islamabad, Abbottabad Campus, Abbottabad – 22060, KPK, Pakistan

[3]Graduate School of Science and Technology, University of Tsukuba, 1-1-1 Tennodai, Tsukuba, Ibaraki, 305–8573 Japan

[4]School of Environment and Resources, Laboratory of Solid Waste Treatment and Resource Recycle, Southwest University of Science and Technology, Mianyang, 621010, China

[5]Department of Biotechnology, COMSATS University Islamabad, Abbottabad Campus, Abbottabad – 22060, KPK, Pakistan

[6]College of Chemical Engineering, Nanjing Tech University, NO. 30 Puzhu South Road(S), Nanjing 211816, PR China

[7]Department of Chemical and Materials Engineering, Northern Border University, Arar, 91431, Kingdom of Saudi Arabia

[8]Department of Civil and Environmental Engineering, College of Engineering, King Faisal University, Al-Ahsa 31982, Saudi Arabia.

Corresponding author:

mbilal@cuiatd.edu.pk (Prof. Dr. Muhammad Bilal[*])

mqdir@kfu.edu.sa (Dr. Muhammad Tahir Amin[***])

ahson@cuiatd.edu.pk (Dr. Ahson Jabbar Shaikh[**])

Supplementary Information

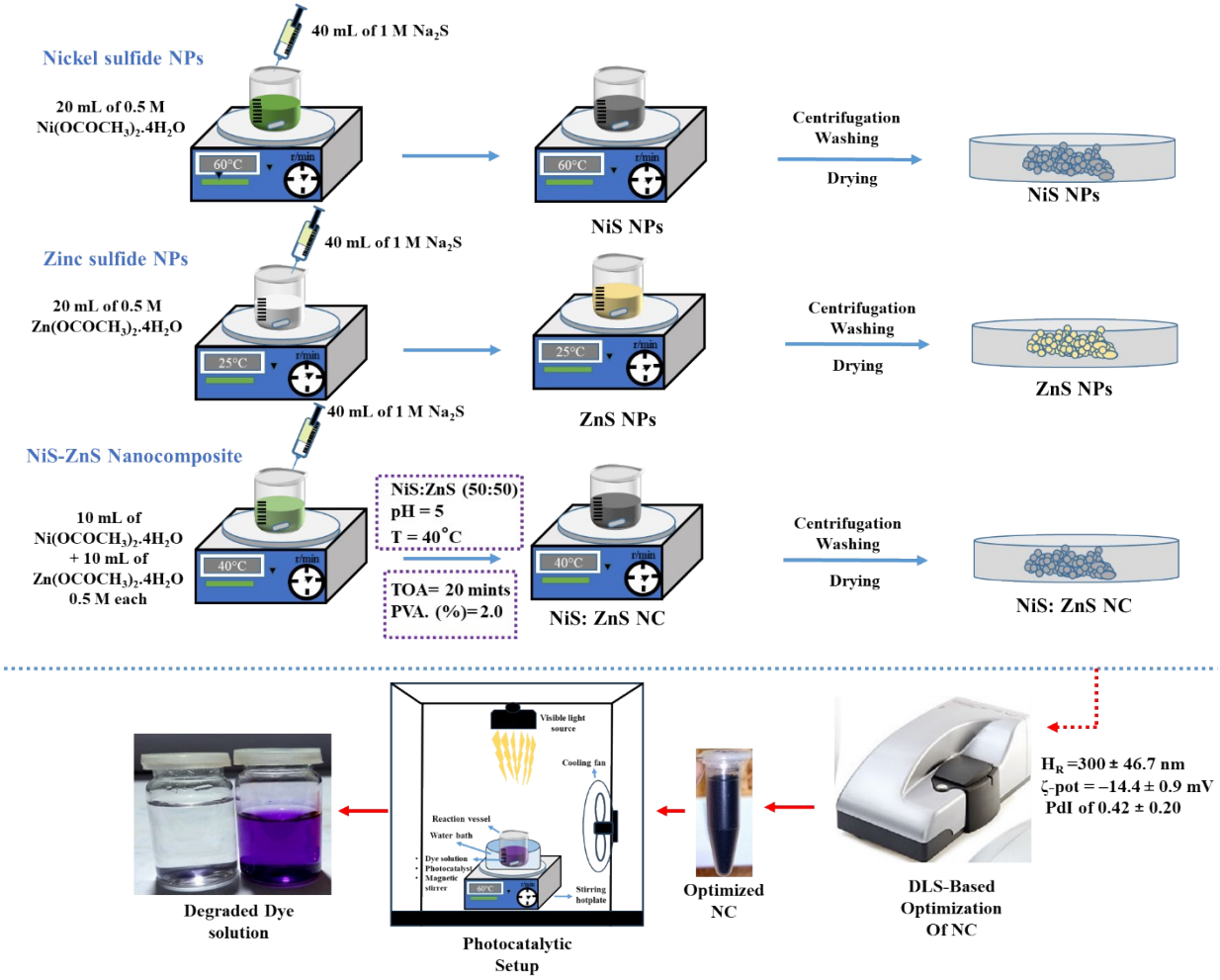

Synthesis Methodology of NiS, ZnS NPs, and NiS-ZnS NC

Fig. S1. Chemical precipitation and co-precipitation methods for the synthesis of NiS, ZnS, and NiS-ZnS nanocomposite, and experimental setup of photocatalytic degradation.

Electron Images and EDX Spectra of NiS-ZnS NC

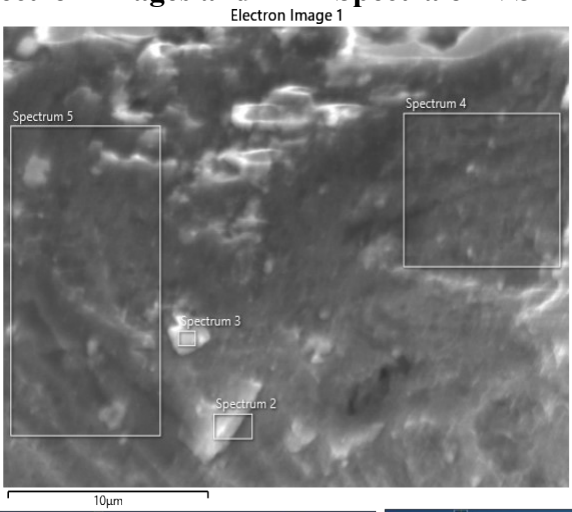

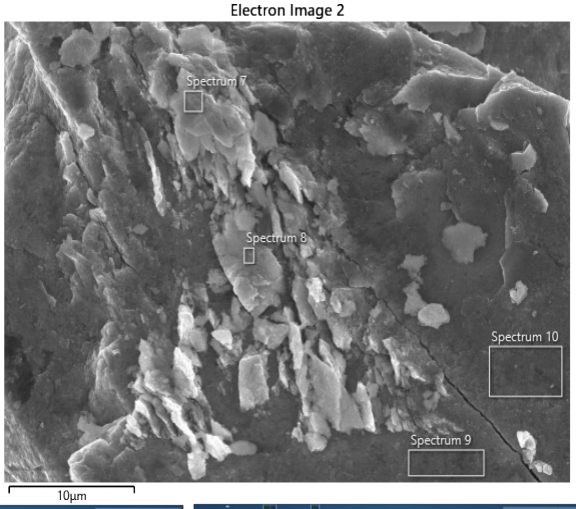

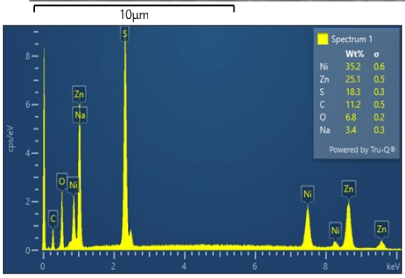

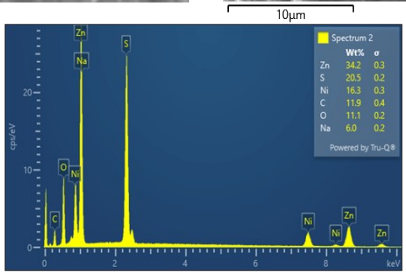

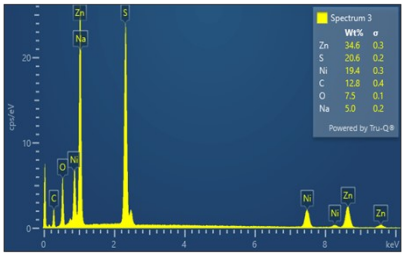

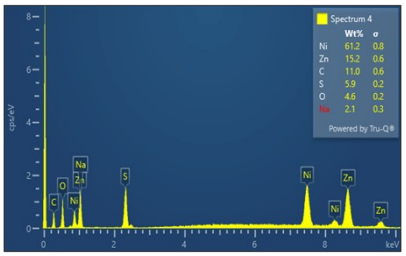

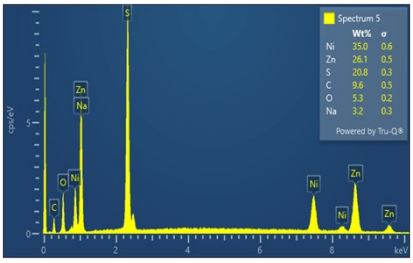

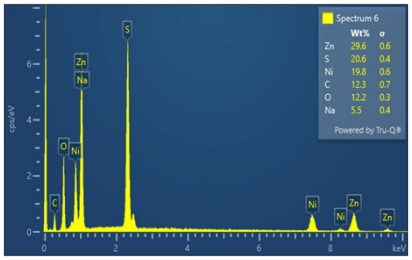

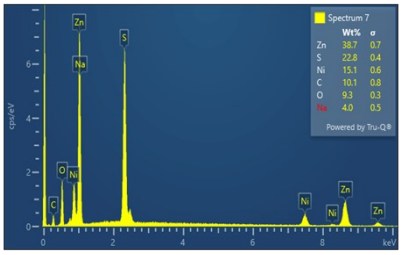

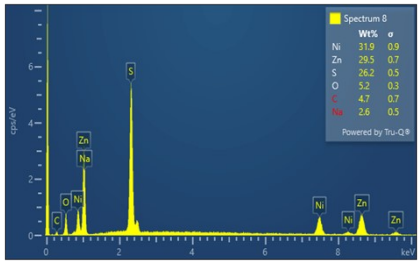

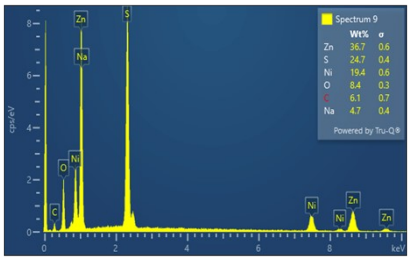

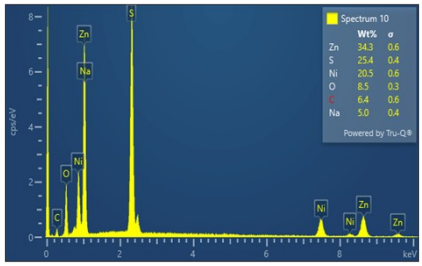

Fig. S2. Electron images and EDX spectra of NiS-ZnS Nanocomposite.

Table S1. EDX results obtained from ten spectra show the weight percentage (%) of each element in the NiS-ZnS nanocomposite. (S = Spectrum)

Element	**S-1 (wt. %)**	**S-2 (wt. %)**	**S-3 (wt. %)**	**S-4 (wt. %)**	**S-5 (wt.%)**	**S-6 (wt. %)**	**S-7 (wt. %)**	**S-8 (wt. %)**	**S-9 (wt. %)**	**S-10 (wt. %)**
Ni	35.2	34.2	34.6	62.1	35.0	29.6	38.7	31.9	36.7	34.3
S	25.1	20.5	20.6	15.2	26.1	20.6	22.8	29.5	24.7	25.4
Zn	18.3	16.3	19.4	11.0	20.8	19.8	15.1	26.2	19.4	20.5
C	11.2	11.9	12.8	5.9	9.6	12.3	10.1	5.2	8.4	8.5
O	6.8	11.1	7.5	4.6	5.3	12.2	9.3	4.7	6.1	6.4
Na	3.4	6.0	5.0	2.1	3.2	5.5	4.0	2.6	4.7	5.0

Photocatalysts	**Weight. %**			**References**
NiS-ZnS Nanocomposite	Ni-37.2%	S-23.05%	Zn-18.7%	**Given Study**
ZnS/NiS Nanocomposite	Ni-44.4%	S-34%	Zn-21.6%	[1]
NiS-ZnS QDs	Ni-20.85%	S-20.85%	Zn-52.71%	[2]

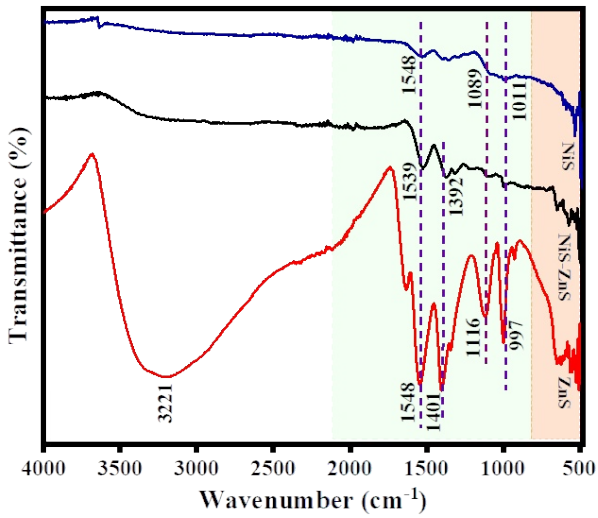

FTIR Spectra of NiS, ZnS, and NiS-ZnS Nanocomposite

Fig. S3. FTIR spectra of pure NiS, ZnS NPs, and optimized NiS-ZnS NC.

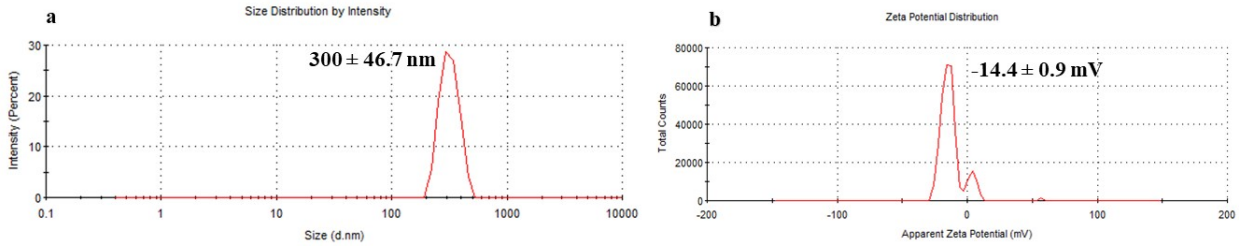

DLS Studies of Optimized NC

Fig. S4. (a) Size distribution, and (b) Zeta potential curve of optimized nanocomposite.

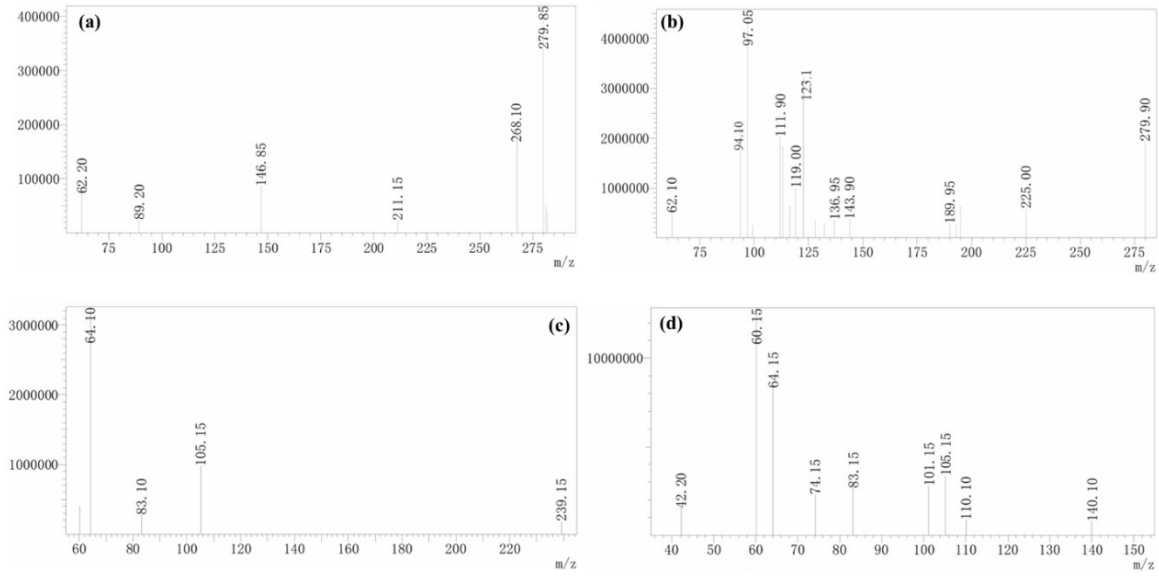

LC-MS Spectra of Crystal Violet dye after Photocatalytic Degradation

Fig. S5. LC-MS chromatogram of the degraded CV solution after 60 minutes.

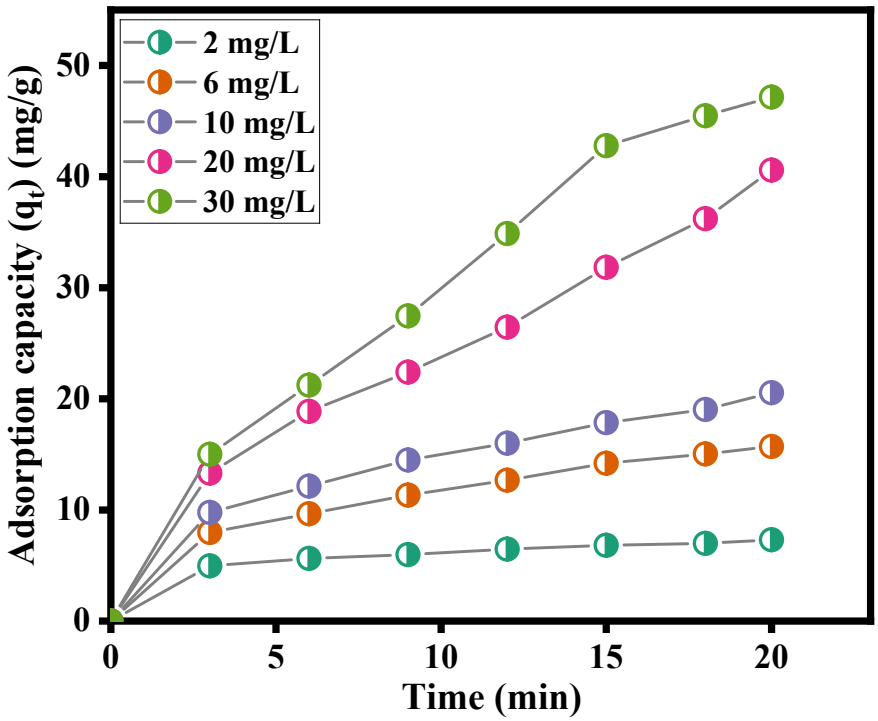

Adsorption Capacity of NiS-ZnS NC for Various Crystal Violet Dye Concentrations

Fig. S6. Effect of initial CV concentration on the adsorption capacity (dose 0.2 g/L, dark reaction time 20 min, pH 6.9, stirring speed = 300 rpm).

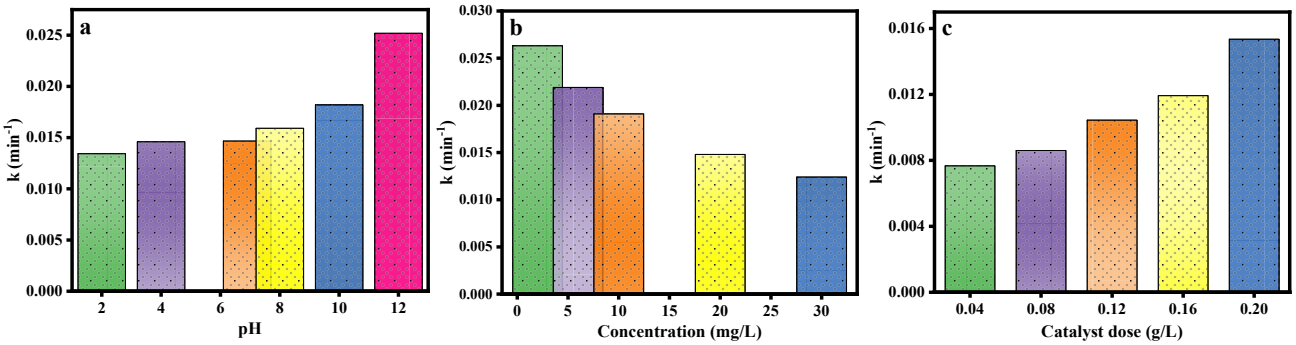

PFO Kinetic Models of pH, Concentration, and Dose Study

Fig. S7. PFO kinetic models' apparent rate constant values, (a) Effect of pH (b) Effect of initial dye concentration (c) Effect of photocatalyst loading.

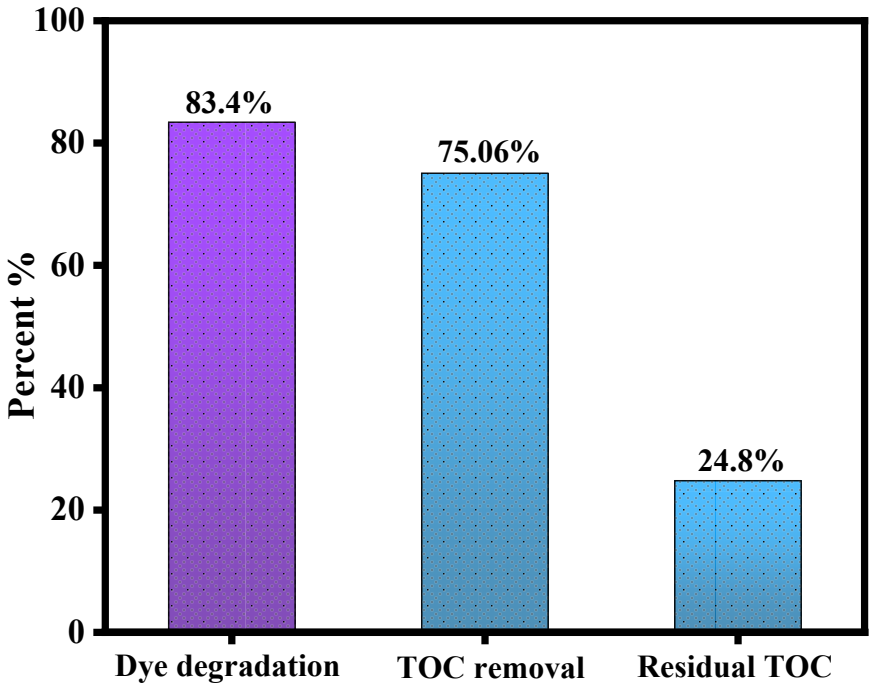

TOC Analysis

Fig. S8. TOC analysis (dose 0.2 g/L, CV concentration 20 mg/L, temp 20°C, pH 6.9).

Table S2**.** The degraded intermediates of CV from the LC-MS chromatogram.

No.	Molecular weight	m/z	Molecular formula	Chemical name	Chemical structures
1	268.10	268.10	$C_{17}H_{20}N_2O$	4-(N,N-dimethylamino)-4′-(N′,N′-dimethylamino)benzophenone	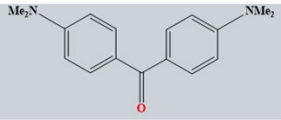
2	240.35	239.15	$C_{15}H_{16}N_2O$	4-(N,N-dimethyl amino)-4′-aminobenzophenone	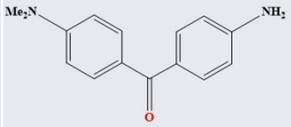
3	226.27	225.00	$C_{14}H_{14}N_2O$	4-(N-methylamino)-4′-aminobenzophenone	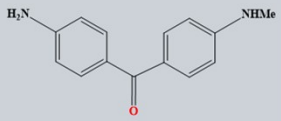
4	212.25	211.15	$C_{13}H_{12}N_2O$	4,4′-Bis-aminobenzophenone	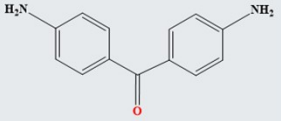
5	137.14	136.95	$C_7H_7NO_2$	4-aminobenzoic acid	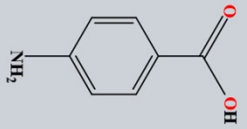
6	137.18	136.95	$C_8H_{11}NO$	4-N,N (dimethyl amino) phenol	
7	123.15	123.1	C_7H_9NO	4-N,N (dimethyl amino) phenol	
8	109.13	110.10	C_6H_7NO	4-aminophenol	
9	93.13	94.10	C_6H_7N	Anline	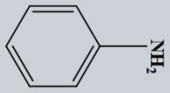
10	74.08	74.15	$C_3H_6O_2$	1-Hydroxypropan-2-one	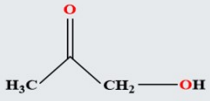
11	62.01	62.20	NO_3^-	Nitrates	NO_3^-
12	60.05	60.10	$C_2H_4O_2$	Acetic acid	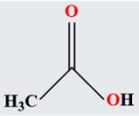
13	60.01	60.10	CO_3^-	Carbonates	CO_3^-
14	43.01	42.20	CH_3CO^+	Acetyl cation	CH_3CO^+

Table S3. The energies of LUMO, HOMO, and bandgap (eV) were calculated using the B3LYP model with the STO-3G basis set.

Materials	**E_{HOMO} (eV)**	**E_{LUMO} (eV)**	**Energy gap (eV)**
NiS	-2.22	-1.60	0.62
ZnS	-2.04	-0.36	1.68
NiS-ZnS	-1.59	-0.17	1.42
Crystal Violet	-1.46	2.88	4.34
NiS-ZnS@CV (C1)	-1.44	0.58	2.02
NiS-ZnS@CV (C2)	-1.42	0.52	1.94

Table S4. Literature comparison of the interactive energy of CV dye with different materials calculated using Eq. 1.

Materials	**Interaction Energy (kcal/mol)**	**References**
SA@6DP + CV	-61.96	[3]
AgNPs@PPC + CV	-95.85	[4]
Watermelon Seeds + CV	-170.25	[5]
Polyacrylamide + CV	-147.95	[6]
Carpobrotus edulis + CV	-170.28	[7]

NiS-ZnS + CV (C1)	-197.27	Our Work
NiS-ZnS + CV (C2)	-199.18	Our Work

Table S5. Hydrodynamic size (H_R) and ζ-potential of NC in salt, after dye adsorption and degradation

DLS studies	**NC**	**$NaNO_3$**	**Na_2SO_4**	**NaCl**	**$CaCl_2$**	**$AgNO_3$**
H_R (Salts)	300.4±40.7	800.9± 50.1	642± 33	659.7± 43	414±15	394± 0.5
ZP (Salts)	-14.4 ±0.9	-10±1.9	-14± 0.85	-11.9±0.5	-6.4±0.16	-16.7± 0.08
H_R (Dye adsorption)		624±249	707±163	834±329	925±302	1625 ±392
H_R (Dye degradation)		366.6±63	422±92	400.05 ±82.5	399±24	477±117
ZP (Dye adsorption)		-11.4 ±1.1	-5 ±0.85	-4.23 ±0.67	2.4±0.2	-4.6± 0.16
ZP (Dye degradation)		-11.05 ±0.65	-12 ±3.2	-10.6± 0.55	-3.4±0.1	-3.93± 1.57

Generation of Hydroxyl Radicals from Nitrate Ions under Visible Light

$$NO_3^- + h\upsilon \rightarrow NO_2^- + O \quad (1)$$

$$NO_3^- + h\upsilon \rightarrow O^{\cdot -} + NO_2^{\cdot} \quad (2)$$

$$NO_2^- + H_2O + h\upsilon \rightarrow NO_2^- + OH^- + {}^{\cdot}OH \quad (3)$$

$$2NO_2^{\cdot} + H_2O \rightarrow NO_2^{-} + NO_3^{-} + 2H^{+} \quad (4)$$

$$O^{\cdot -} + H_2O \rightarrow {}^{\cdot}OH + HO^{-} \quad (5)$$

$$O + H_2O \rightarrow 2^{\cdot}OH \quad (6)$$

Generation of Oxygen and Hydroxyl Radical from Nitrate Ions

$$NO_3^{-} + light \rightarrow NO_3^{\cdot -} \rightarrow NO_2^{-} + O^{\cdot -} \quad (7)$$

$$O^{\cdot -} + H_2O \rightarrow \cdot OH + OH^{-} \quad (8)$$

$$NO_2^{-} + \cdot OH \rightarrow \cdot NO_2 + OH^{-} \quad (9)$$

Generation of Chloride Radical

$$Cl^{-} + h\nu_B \rightarrow Cl^{\cdot} \quad (10)$$

$$Cl^{\cdot} + Cl^{-} \rightarrow Cl_2^{\cdot -} \quad (11)$$

Generation of Sulfate Radical

$$SO_4^{2-} + h^{+} \rightarrow SO_4^{\cdot -} + OH^{-} \quad (12)$$

$$SO_4^{\cdot -} + e^{-}cb \rightarrow SO_4^{2-} \quad (13)$$

Generation of Chloride Radical

$$\cdot OH + Cl^{-} \leftrightharpoons ClOH^{\cdot -} \quad (14)$$

$$ClOH^{\cdot -} + H^{+} \leftrightharpoons H_2O + Cl\cdot \quad (15)$$

$$Cl\cdot + Cl^{-} \leftrightharpoons Cl_2^{\cdot -} \quad (16)$$

$$Cl_2.^- + Cl_2.^- \rightarrow Cl_2 + 2Cl^- \quad (17)$$

$$Cl_2 + H_2O \rightarrow HClO + H^+ + Cl^- \quad (19)$$

References

1. Amiri, F., et al., *Detailed investigation of the optical and photocatalytic properties of ZnS/NiS nanocomposite for efficient water purification and dye degradation.* International Journal of Environmental Science and Technology, 2026. **23**(1): p. 48.
2. Alagarsamy, V., et al., *NiS-ZnS quantum dots as visible-light photocatalysts for enhanced dye degradation in sustainable wastewater treatment.* Chemical Physics Impact, 2025: p. 100912.
3. Mokhtar, A., et al., *Removal of crystal violet dye using a three-dimensional network of date pits powder/sodium alginate hydrogel beads: Experimental optimization and DFT calculation.* International Journal of Biological Macromolecules, 2023. **251**: p. 126270.
4. Kamal, A.-b., et al., *Developing a cost-effective and eco-friendly adsorbent/photocatalyst using biomass and urban waste for crystal violet removal and antimicrobial applications.* Biomass Conversion and Biorefinery, 2025. **15**(7): p. 10089-10107.
5. Elboughdiri, N., et al., *Application of statistical physical, DFT computation and molecular dynamics simulation for enhanced removal of crystal violet and basic fuchsin dyes utilizing biosorbent derived from residual watermelon seeds (Citrullus lanatus).* Process Safety and Environmental Protection, 2024. **186**: p. 995-1010.
6. Lebkiri, I., et al., *Investigation of the anionic polyacrylamide as a potential adsorbent of crystal violet dye from aqueous solution: Equilibrium, kinetic, thermodynamic, DFT, MC and MD approaches.* Journal of Molecular Liquids, 2023. **372**: p. 121220.
7. Dabagh, A., et al., *Application of Taguchi method, response surface methodology, DFT calculation and molecular dynamics simulation into the removal of orange G and crystal violet by treated biomass.* Heliyon, 2023. **9**(11).